PRECONDITIONED LARGE-EDDY SIMULATIONS FOR TUNDISH FLOWS

Nouri A. Alkishriwi, Matthias Meinke, and Wolfgang Schröder
Aerodynamisches Institut, RWTH Aachen,
Wüllnerstraße zw. 5 und 7, D-52062 Aachen, Germany
nouri@aia.rwth-aachen.de

ABSTRACT

Large-eddy simulations (LES) of a continuous tundish flow are carried out to investigate the turbulent flow structure and vortex dynamics. The numerical computations are performed by solving the viscous conservation equations for compressible fluids. An implicit dual time stepping scheme combined with low Mach number preconditioning and a multigrid accelerating technique is developed for LES computations. The method is validated by comparing data of turbulent pipe flow at $Re_\tau = 1280$ and cylinder flow at Re = 3900 at different Mach numbers with experimental findings from the literature. Finally, the characteristics of the flow in a one-strand tundish is analyzed.

INTRODUCTION

In many engineering problems compressible and nearly incompressible flow regimes occur simultaneously. For example low speed flows, which may be compressible due to surface heat transfer or volumetric heat addition. The numerical analysis of such flows requires to solve the viscous conservation equations for compressible fluids to capture the essential effects.

When a compressible flow solver is applied to a nearly incompressible flow, its performance can deteriorate in terms of both speed and accuracy (Turkel, 1999). It is well known that most compressible codes do not converge to an acceptable solution when the Mach number of the flow field is smaller than $\mathcal{O}(10^{-1})$. The main difficulty with such low speed flows arises from the large disparity between the wave speeds. The acoustic wave speed is $|u\pm c|$, while entropy or vorticity waves travel at $|u|$, which is quite small compared to $|u\pm c|$. In explicit time-marching codes, the acoustic waves define the maximum time step, while the convective waves determine the total number of iterations such that the overall computational time becomes large for small Mach numbers.

Different methods have been proposed to solve such mixed flow problems by modifying the existing compressible flow solvers. One of the most popular approaches is to use low Mach number preconditioning methods for compressible codes (Turkel, 1999). The basic idea of this approach is to modify the time marching behavior of the system of equations without altering the steady state solution. This is, however, only useful when the steady state solution is sought. A straightforward extension of the preconditioning approach to unsteady flow problems is achieved when it is combined with a dual time stepping technique.

This idea is followed in the present paper, i.e., a highly efficient large-eddy simulation method is described based on an implicit dual time stepping scheme combined with preconditioning and multigrid. This method is validated by well-known case studies Alkishriwi et al. (2004) and finally, the preconditioned large-eddy simulation method is used to investigate the flow field in a continuous casting tundish.

In continuous casting of steel, the tundish enables to remove nonmetallic inclusions from molten steel and to regulate the flow from individual ladles to the mold. There is two types of flow conditions in a tundish: steady-state casting where the mass flow rate through the shroud m_{sh} is equal to the mass flow rate through the submerged entry nozzle into the mold m_{SEN}, and transient casting in which the mass of steel in a tundish varies in time during the filling or draining stages. The motion of the liquid steel is generated by jets into the tundish and continuously casting mold. The flow regime is mostly turbulent, but some turbulence attenuation can occur far from the inlet. The characteristics of the flow in a tundish include jet spreading, jet impingement on the wall, wall jets, and an important decrease of turbulence intensity in the core region of the tundish far from the jet (Gardin et al. 1999) and (Odental et al. 2002).

In previous studies, a large amount of research has been carried out to understand the physics of the flow in a tundish mainly through numerical simulations based on the Reynolds-averaged Navier–Stokes (RANS) equations plus an appropriate turbulence model. To gain more knowledge about the transient turbulence process, which cannot be achieved via RANS solutions, large-eddy simulations of the tundish flow field are performed.

After a concise presentation of the governing equations the implementation of the preconditioning in the LES context using the dual time stepping technique is described. Then, the discretization and the time marching solution technique within the dual time stepping approach are discussed. After the description of the boundary conditions and the computational domain of the tundish flow, the numerical results of the validation cases and the tundish simulation are presented.

GOVERNING EQUATIONS

The governing equations are the unsteady three-dimensional compressible Navier-Stokes equations written in generalized coordinates $\xi_i, i = 1, 2, 3$

$$\frac{\partial \mathbf{Q}}{\partial t} + \frac{\partial (\mathbf{F}_{c_i} - \mathbf{F}_{v_i})}{\partial \xi_i} = 0 \quad , \tag{1}$$

where the quantity $\mathbf{Q}$ represents the vector of the conservative variables and $\mathbf{F}_{c_i}$, $\mathbf{F}_{v_i}$ are inviscid and viscous flux vectors, respectively. As mentioned before, preconditioning is required to provide an efficient and accurate method of solution of the steady Navier–Stokes equations for compressible flow at low Mach numbers. Moreover, when unsteady flows are considered, a dual time stepping technique for time accurate

solutions is used. In this approach, the solution at the next physical time step is determined as a steady state problem to which preconditioning, local time stepping and multigrid are applied.

Introducing of a pseudo-time τ in (1), the unsteady two-dimensional governing equations with preconditioning read

$$\mathbf{\Gamma}^{-1}\frac{\partial \mathbf{Q}}{\partial \tau} + \frac{\partial \mathbf{Q}}{\partial t} + \mathbf{R} = 0, \tag{2}$$

where $\mathbf{R}$ represents

$$\mathbf{R} = \left(\frac{\partial \mathbf{E}_c}{\partial \xi} + \frac{\partial \mathbf{F}_c}{\partial \eta} + \frac{\partial \mathbf{E}_v}{\partial \xi} + \frac{\partial \mathbf{F}_v}{\partial \eta}\right) \tag{3}$$

and $\mathbf{\Gamma}^{-1}$ is the preconditioning matrix, which is to be defined such that the new eigenvalues of the preconditioned system of equations are of similar magnitude. In this study, a preconditioning technique from Turkel (1999) has been implemented. It is clear that only the pseudo-time terms in (2) are altered by the preconditioning, while the physical time and space derivatives retain their original form. Convergence of the pseudo-time within each physical time step is necessary for accurate unsteady solutions. This means, the acceleration techniques such as local time stepping and multigrid can be immediately utilized to speed up the convergence within each physical time step to obtain an accurate solution for unsteady flows. The derivatives with respect to the physical time t are discretized using a three-point backward difference scheme that results in an implicit scheme, which is second-order accurate in time

$$\frac{\partial \mathbf{Q}}{\partial \tau} = \mathbf{RHS} \tag{4}$$

with the right-hand side

$$\mathbf{RHS} = -\mathbf{\Gamma}\left(\frac{3\mathbf{Q}^{n+1} - 4\mathbf{Q}^{n} + \mathbf{Q}^{n-1}}{2\Delta t} + \mathbf{R}(\mathbf{Q^{n+1}})\right) \quad .$$

Note that at $\tau \rightarrow \infty$ the first term on left-hand side of (2) vanishes such that (1) is recovered. To advance the solution of the inner pseudo-time iteration, a 5-stage Runge-Kutta method in conjunction with local time stepping and multigrid is used. For stability reasons the term $\frac{3\mathbf{Q}^{n+1}}{2\Delta t}$ is treated implicitly within the Runge-Kutta stages yielding the following formulation for the l^{th} stage

$$\begin{aligned} \mathbf{Q^0} &= \mathbf{Q^n} \\ &\vdots \\ \mathbf{Q^l} &= \mathbf{Q^0} - \alpha_l \Delta\tau \left[\mathbf{I} + \frac{3\Delta\tau}{2\Delta t}\alpha_l \mathbf{\Gamma}\right]^{-1} \mathbf{RHS} \\ &\vdots \\ \mathbf{Q^{n+1}} &= \mathbf{Q^5}. \end{aligned} \tag{5}$$

The additional term means that in smooth flows the development in pseudo-time is proportional to the evolution in t.

NUMERICAL PROCEDURE

The governing equations are the NAVIER–STOKES equations filtered by a low-pass filter of width Δ, which corresponds to the local average in each cell volume. The monotone integrated large-eddy simulations (MILES) approach is used to implicitly model the small scale motions through the numerical scheme.

The approximation of the convective terms of the conservation equations is based on a modified second-order accurate AUSM scheme using a centered 5-point low dissipation stencil Meinke et al. (2002) to compute the pressure derivative in the convective fluxes. The pressure term contains an additional expression, which is scaled by a weighting parameter χ that represents the rate of change of the pressure ratio with respect to the local Mach number. This parameter determines the amount of numerical dissipation to be added to avoid oscillations that could lead to unstable solutions. The parameter χ was chosen in the range $0 \leq \chi \leq \frac{1}{400}$. The viscous stresses are discretized to second-order accuracy using central differences, i.e., the overall spatial approximation is second-order accurate.

A dual time stepping technique is used for the temporal integration. In this approach, the solution at the next physical time step is determined as a steady state problem to which preconditioning, local time stepping and multigrid are applied. A 5-stage Runge-Kutta method is used to propagate the solution from time level n to n+1. The Runge-Kutta coefficients $\alpha_l = (\frac{6}{24}, \frac{4}{24}, \frac{9}{24}, \frac{12}{24}, \frac{24}{24})$ are optimized for maximum stability of a centrally discretized scheme. The physical time derivative is discretized by a backward difference formula of second-order accuracy. The method is formulated for multi-block structured curvilinear grids and implemented on vector and parallel computers.

TUNDISH FLOW

In the following the numerical setup of the tundish flow is briefly described. The geometry and the flow configuration for the simulation are shown in Fig. 1.

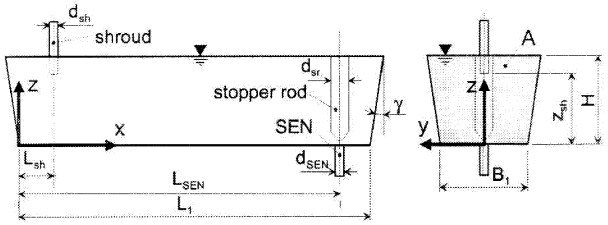

Figure 1: Presentation of the main parameters of the tundish geometry.

The numerical simulations consist of two simultaneously performed computations on the one hand, the pipe flow is calculated to provide time-dependent inflow data for the jet into the tundish and on the other hand, the flow field within the tundish. The geometrical values and the flow parameters of the tundish are given in Table 1. The computational domain is discretized by 12 million grid points, 5 million of which are located in the jet domain to resolve the essential turbulent structures. Since the jet possesses the major impact on the flow characteristics in the tundish, it is a must to determine in great detail the interaction between the jet and the tundish flow.

Table 1: Physical parameters of the tundish flow.

tundish length L_1	1.847 m
tundish width B_1	0.459 m
tundish height H	0.471 m
inclination of side walls	7^o
diameter of the shroud d_{sh}	0.04 m
height between bottom shroud Z_{sh}	0.352 m
diameter of the SEN d_{SEN}	0.041 m
diameter of the stopper rod d_{sr}	0.0747 m
hydraulic diameter d_{hyd}	0.6911 m
Re based on the jet diameter	25000

The boundary conditions consist of no-slip conditions on solid walls. At the free surface, the normal velocity components and the normal derivatives of all remaining other variables are set zero. An LES of the impinging jet requires a prescription of the instantaneous flow variables at the inlet section of the jet. To determine those values a slicing technique based on a simultaneously conducted LES of a fully developed turbulent pipe flow is used.

VALIDATION

To validate the efficiency and the accuracy of the method, large-eddy simulations of turbulent pipe flow at a Reynolds number $Re_\tau = 1280$ based on the friction velocity u_τ, which corresponds to a diameter D based Reynolds number $Re_D = u_{cl}D/\nu = 22550$, are investigated. The Mach number based on the centerline velocity of the pipe is set to $Ma = 0.02$ and the physical time step $\Delta t = 0.01$. The comparison of the pure explicit LES results from Rütten et al. (2001 & 2005) and the LES findings of the implicit method in Figs. 2 and 3 shows a good agreement for the mean velocity profiles and the turbulence intensity distributions.

The flow around a cylinder at a diameter based $Re_D = 3900$ is performed at a freestream Mach number $M_\infty = 0.05$ and a physical time step $\Delta t = 0.02$. Figure 4 shows the streamwise velocity distribution on the centerline in the wake of the cylinder compared with the LES distribution of a pure explicit scheme without preconditioning at a Mach number $M_\infty = 0.1$ and with experimental data from the literature. The profiles of the velocity fluctuations of the streamwise and vertical components at $X/D = 1.54$ as a function of Y/D presented in Figs. 5 and 6 corroborate the correspondence with the measurements from Lourenco and Shih (1994).

The efficiency analysis is performed for different parameters such as the size of the physical time step, the required residual constraint for the inner pseudo-time iteration, the Mach number and the Reynolds number. Figs. 7 and 8 demonstrate the impact of the size of the physical time step and the Mach number on the efficiency of the implicit scheme. It is evident that as the size of the physical time step increases, the required number of iterations in the inner pseudo-time cycle grows. Fig. 8 demonstrates the impact of the Mach number on the efficiency of the implicit scheme. The results, which are based on the simulations of turbulent channel flow at $Re_\tau = 590$ and $Ma = 0.01$, show a speedup in the range of 9 to 60 compared to the explicit scheme for a reduction of two orders of magnitude. Note, that for a reduction of three orders of magnitude this speedup is lowered to a range of 6 to 26.

RESULTS

The typical structure of the velocity field in the tundish is shown in Figs. 9-15. These figures show the computed flow pattern in different locations within the tundish. Figs. 9 to 12 visualize the jet flow into the tundish. It is clear that the turbulent flow contains a wide range of length scales. Large eddies with a size comparable to the diameter of the pipe occur together with eddies of very small size. The figures evidence the jet spreading, jet impingement on the wall, and wall jets. The jet ejected from the ladle reaches the bottom of the tundish at high velocities, spreads in all directions and then mainly flows along the side walls of the tundish. This behavior can be seen in Figs. 12 and 14. Such a flow pattern leads to nonmetallic inclusions, which are to be avoided.

Figs. 13 and 14 represent flow field structures in the center and near-wall longitudinal vertical planes of the tundish. The streamlines in these figures illustrate the vortex dominated flow in the tundish. It can be seen that the flow includes strong vortices and recirculation regions mainly in the inlet region of the tundish, which is fully turbulent. In Fig. 15 the turbulent jet flow in a tundish is visualized by the λ_2 criterion.

CONCLUSION

An efficient large-eddy simulation method for nearly incompressible flows based on solutions of the governing equations of viscous compressible fluids has been introduced. The method uses an implicit time accurate dual time-stepping scheme in conjunction with low Mach number preconditioning and multigrid acceleration. To validate the scheme, large-eddy simulations of turbulent pipe flow at $Re_\tau = 1280$, and cylinder flow at $Re_D = 3900$ have been performed. The results show the scheme to be efficient and to improve the accuracy at low Mach number flows. Generally, the new method is 6-40 times faster than the basic explicit 5-stage Runge-Kutta scheme.

A large-eddy simulation of the flow field in a tundish is conducted to analyze the flow structure, which determines to a certain extent the steel quality. The findings evidence many intricate flow details that have not been observed before by customary RANS approaches.

REFERENCES

Alkishriwi, N., Meinke, M., W. Schröder, W., 2004, "Efficient Large-eddy simulation of low Mach number flow", Presented in 14^{th} -DGLR Symposium der STAB, Nov. 16-18, 2004, Bremen, Germany.

Alkishriwi, N., Meinke, M., Schröder, W., 2004, "A Large-eddy simulation method for low Mach number flows using preconditioning and multigrid", Submitted to *Computers and Fluids*.

Beaudan, P., and Moin, P., 1994, "Numerical experiments on the flow past a circular cylinder at sub-critical Reynolds numbers", Technical Report TF-62, Center Turb. Res., Stanford.

Durst, F., Jovanovic, J., Sender, J., 1995, "LDA measurement in the near-wall region of a turbulent pipe flow", *J. Fluid Mech.*, 295:305-335.

Gardin, P., Brunet, M., Domgin, J. F., and Pericleous, K., 1999," An Experimental and numerical CFD study of turbulence in a tundish container", *Second International Conference on CFD in the Minerals and Process Industries CSIRO*, Melbourne, Australia, 6-8 December.

Lourenco, L. M., and Shih., C., 1993, "Characteristics of the plane turbulent near wake of a circular cylinder", A particle image velocimetry study. (Data taken from Beaudan and Moin, 1994).

Meinke, M., Schröder, W., Krause, E., and Rister, T., 2002, "A comparison of second- and sixth-order methods for large-eddy simulations", *Comp. & Fluids*, Vol. 31, pp. 695-718.

Odenthal, H., Bölling, R., and Pfeifer, H., 2002, " Numerical and physical simulation of tundish fluid flow phenomena", 11^{th} *Japan-Germany Seminar on Fundamentals of Iron and Steelmaking*, Düsseldorf.

Rütten, F., Meinke, M., and Schröder, W., 2001, "Large-eddy simulation of 90-pipe bend flows", *J. of Turbulence*, 2, 003.

Rütten, F., Schröder, W., and Meinke, M., 2005, "LES of low frequency oscillation of the Dean vortices in turbulent pipe bend flows", *Physics of Fluids*, Vol. 17, issue 2.

Turkel, E., 1999, "Preconditioning techniques in computational fluid dynamics", *Annual Review of Fluid Mechanics* 31:385-416.

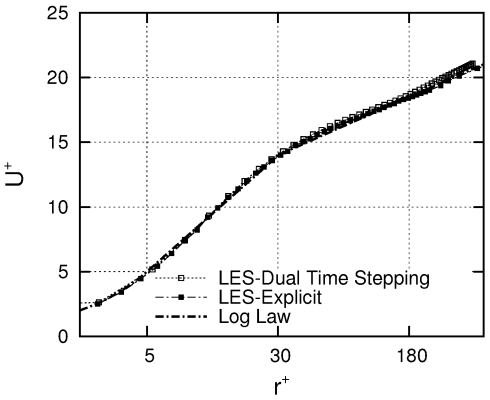

Figure 2: Mean velocity distributions of turbulent pipe flow at Re_τ=1280.

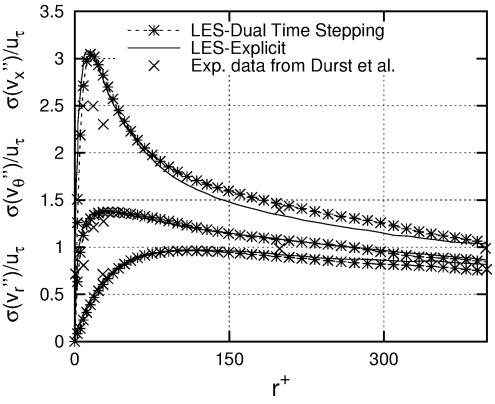

Figure 3: Turbulence intensity distributions of turbulent pipe flow at Re_τ=1280.

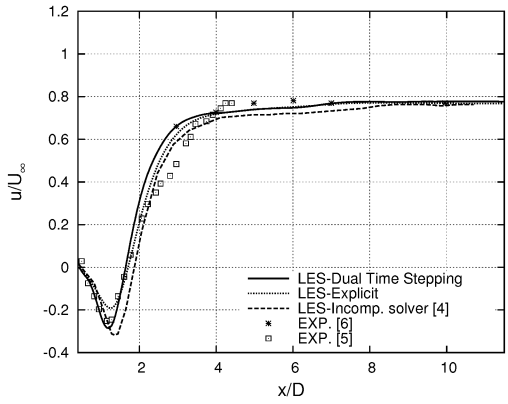

Figure 4: Streamwise velocity as a function of X/D on the centerline $Y/D = 0$, $Z/D = 0$ in the cylinder wake at Re_D = 3900.

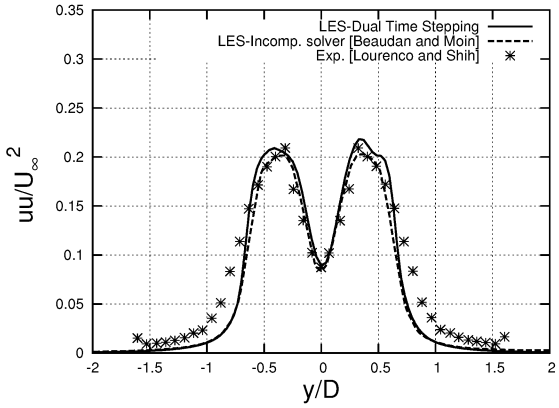

Figure 5: Streamwise velocity fluctuations as a function of Y/D in the cylinder wake at $X/D = 1.54$.

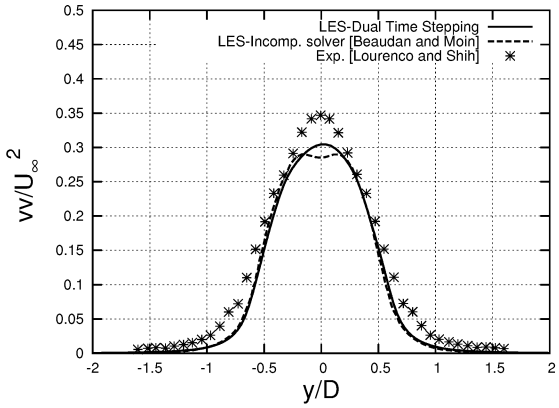

Figure 6: Vertical velocity fluctuations as a function of Y/D in the cylinder wake at $X/D = 1.54$.

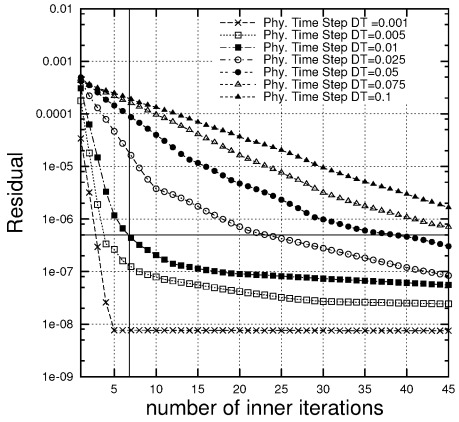

Figure 7: Convergence of the inner iterations at $Ma = 0.01$ for channel flow computations at Re_τ=590.

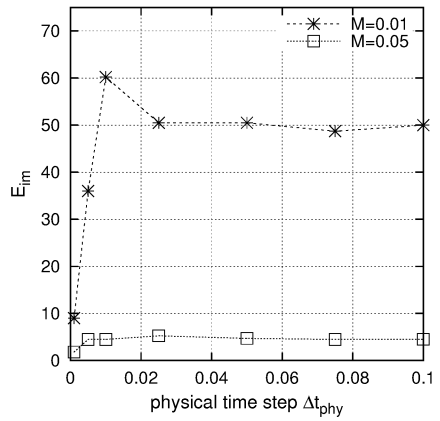

Figure 8: Efficiency E_{im} as a function of Δt_{phy} at $Ma = 0.01$ and $Ma = 0.05$ for channel flow computations at Re_τ=590.

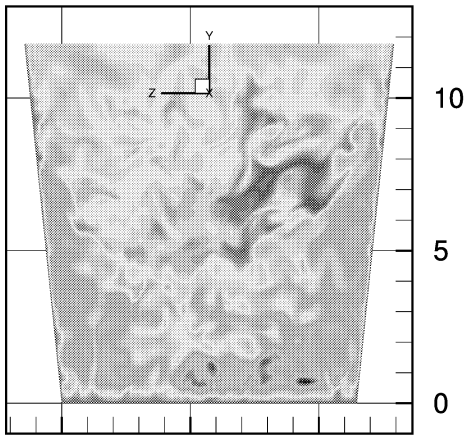

Figure 9: Instantaneous entropy contours at X/L_1=0.

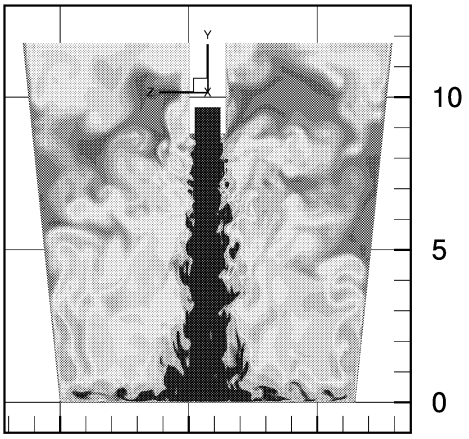

Figure 10: Instantaneous entropy contours in the center plane of the jet.

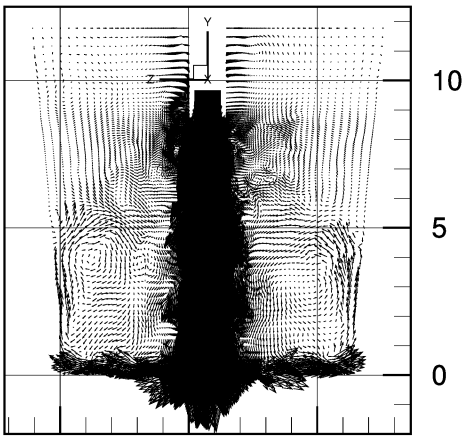

Figure 11: Instantaneous velocity vectors in the center plane of the jet.

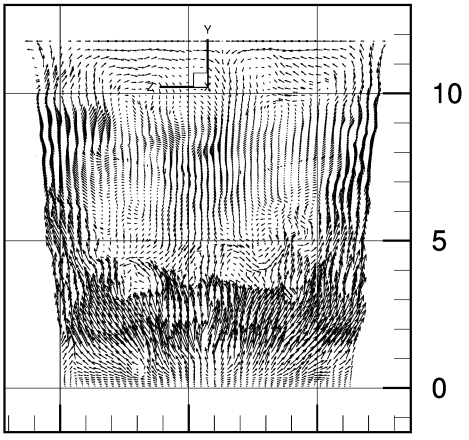

Figure 12: Instantaneous velocity vectors at X/L_1=0.

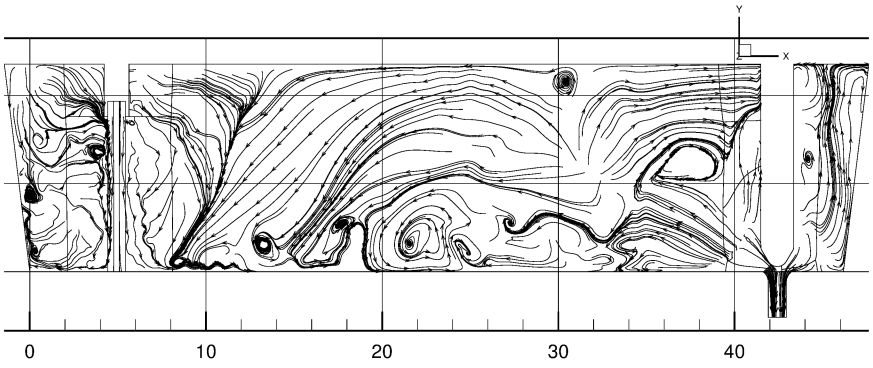

Figure 13: Streamlines at $Z/B_1 = 0$.

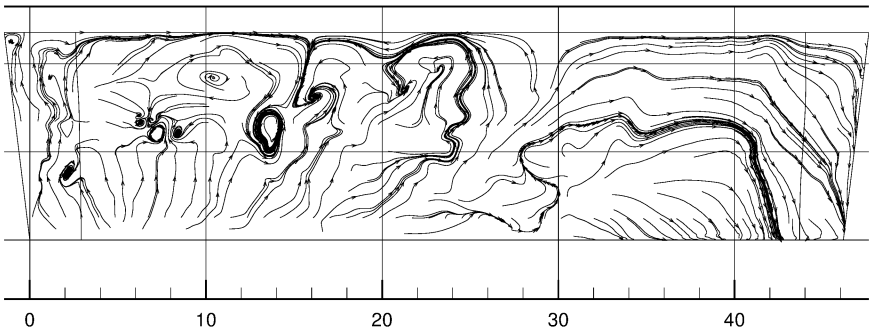

Figure 14: Streamlines near the outer wall.

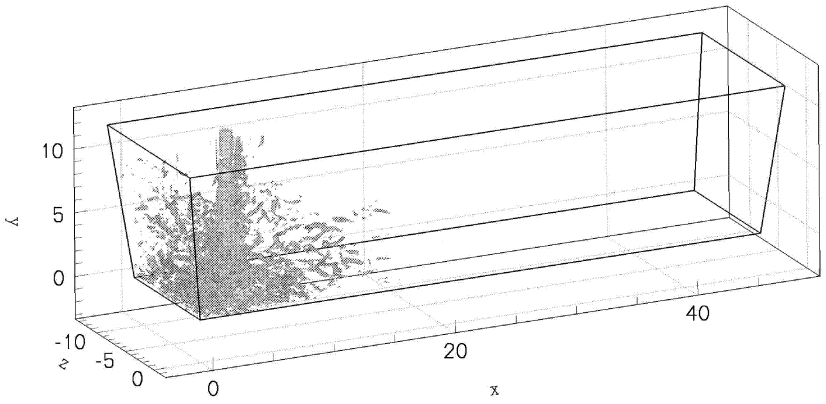

Figure 15: λ_2 contours of the injected jet.